arXiv:cond-mat/0006329v2 [cond-mat.mes-hall] 18 Jul 2000

Pipeline model of a Fermi–sea electron pump

Fernando Sols
Dpto. de Física Teórica de la Materia Condensada, C-V and Instituto de Ciencia de Materiales "Nicolás Cabrera", Universidad Autónoma de Madrid, E-28049 Madrid, Spain

Mathias Wagner*
Hitachi Cambridge Laboratory, Madingley Road, Cambridge CB3 0HE, United Kingdom
(Dated: February 1, 2008)

The use of a band offset between the two leads of an electron pump driven by a local oscillating voltage is shown to increase the pump current dramatically. The structure of the electron transmission suggests the existence of dominant inelastic channels which we call pipelines. This permits the formulation of a simple model that gives a physical account of the numerical results for a realistic device. A spectral analysis reveals the pump current to be carried by scattering states with initial energy deep within the Fermi sea and not at its surface, thereby rendering the effect insensitive to temperature. We show this is compatible with the current flowing near the Fermi surface in the leads.

PACS numbers: 73.40.Ei, 73.50.Pz, 72.40.+w, 05.60.Gg, 73.40.Gk

I. INTRODUCTION

An electron pump stimulates directed electron motion by locally acting on the electron system. This current rectification is achieved by combining nonlinear ac driving with either absence of inversion symmetry in the device, or lack of time-reversal symmetry in the ac signal. The range of possible electron pumps includes the Thouless pump [1, 2] based on Archimedes' water pump, driven quantum-dots [3], electron turnstiles [4], and the recently proposed Fermi-sea pump [5], which makes essential use of a band offset between the two leads. An electron pump may be viewed as a localized version of a ratchet [6, 7, 8] that has been stripped of its spatial periodicity, leaving nonlinearity and asymmetry as the only ingredients responsible for rectified electron motion. Here the role of quantum dissipation [9] is played by the lack of phase coherence between the incoming scattering channels in the left and right leads.

In Ref. [5], we studied an electron pump whose schematic band diagram is shown in panel A of Fig. 1. In this model, a quantum well is driven harmonically by an external ac potential $V_{\rm ac}\cos\omega t$ provided, for instance, by some external gates. Adjacent to the well is a static barrier, and the overall potential profile features a band offset ΔV between the left and right leads. One should note that this band offset is *not* an external bias but rather is due to, for instance, different materials used. The chemical potentials in the contacts to the left and right are taken to be the same. Any dc current flowing is thus due to the effect of the driving ac force alone. It was noted by us [5] that the spatial asymmetry of the model, in particular the band offset ΔV, is vital for a large pump current to exist — boosting it by as much as three orders of magnitude. Crucially, we found the pump current to be carried by electrons with their initial energy narrowly distributed over a fixed interval approximately $\hbar\omega$ wide which, for sufficiently high Fermi energies, may stay well below the Fermi surface, thereby rendering the total current insensitive to temperature. The physical explanation for this peculiar behavior lies in the structure of *pipelines* displayed by the total transmission probability of the device [5]. Pipelines are pairs of left and right scattering channels, of dissimilar energies $E_1 \neq E_2$, that are strongly coupled. Thus, an electron coming, say, from the left with energy E_2 has a relatively high probability of being transmitted to the right with energy $E_1 < E_2$ (see Fig. 1). In the most important cases, $E_2 = E_1 + \hbar\omega$. Due to time-reversal symmetry, $V_{\rm ac}(z,t) = V_{\rm ac}(z,-t)$, these pipelines obey microreversibility: The probability for an electron to go from E_2 to E_1 can be proved to be the same as for the reverse process, i.e., $T_{\rightarrow}(E_1,E_2) \equiv T_{\leftarrow}(E_2,E_1)$.

We further showed that a good deal of the device physics can be explained in terms of the pipeline structure. In particular, one may assume the existence of a single pipeline and reproduce analytically many of the transport features obtained from a sophisticated numerical calculation. The purpose of this paper is to explore this pipeline model in further detail by performing an analytical study that leads to a deeper understanding of the physics involved. In particular, we analyze the different ways in which the total pump current can be decomposed spectrally. As in

*wagner@phy.cam.ac.uk

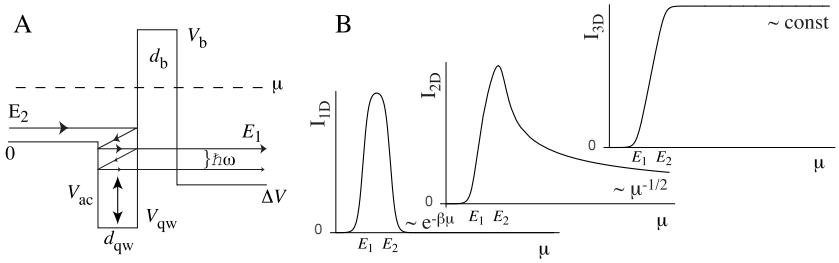

FIG. 1: A: Schematic potential profile for a Fermi-sea pump. The chemical potential μ is the same in both contacts. B: Pump currents in 1, 2, and 3 spatial dimensions as a function of the chemical potential μ for fixed driving as determined by a single–pipeline model.

Ref. [5], we will discuss the properties of the model shown in Fig. 1 in 1, 2 and 3 spatial dimensions, assuming separability of the Hamiltonian $H(t) = -(\hbar^2/2m)\Delta + V_0(z) + V_{\rm ac}(z,t)$.

To evaluate the electronic current, we need to determine the scattering states in the presence of the driving field. Broadly, these states fall into two classes: Scattering states with longitudinal kinetic energy E_z in the incident channel much larger than the photon energy $\hbar\omega$ of the driving field are far away from the conduction band edge, and hence will be insensitive to fine details such as band offset or the presence of a shallow quantum well. Consequently, these states will not contribute to a net pump current, which is in agreement with a recent analysis of pumps in this regime [10]. This is the more commonly studied regime. However, scattering states with *small* longitudinal kinetic energies of the order of $\hbar\omega$ are very sensitive to changes in the band profile and, in particular, have a high probability of the electron getting trapped in the quantum well. The underlying mechanism is that an electron incident, say, from the left with an energy E_2 less than $\hbar\omega$ may, upon reflection at the barrier, emit a photon and thus lose sufficient energy to get caught in the quantum well. Unless it subsequently manages to absorb another photon, the only chance to escape from the quantum well is by tunneling to the right at energy $E_1 = E_2 - \hbar\omega$. This is the mechanism underlying the structure of asymmetric pipelines depicted in panel A of Fig. 1.

In Sect. II we present the pipeline model and derive some of its analytical properties, deferring the spectral properties of the current within this model to Sect. III. In Sect. IV we discuss numerical results for a realistic device and compare them with the analytical predictions of Sects. II and III. Section V contains a summary and some conclusions.

II. THE PIPELINE MODEL

Consider a single pipeline of strength T_p connecting the energies E_1 on the right and E_2 to the left. Assuming incident electrons approaching the device outside these two channels to be reflected with unit probability, we write for the scattering probabilities

$$T_{\rm LR}(E_z, E_z') = T_p \delta(E_z - E_2)\delta(E_z' - E_1) \quad (1)$$
$$T_{\rm RL}(E_z, E_z') = T_p \delta(E_z - E_1)\delta(E_z' - E_2) \quad (2)$$
$$R_{\rm LL}(E_z, E_z') = \delta(E_z - E_z') - T_p \delta(E_z - E_2)\delta(E_z' - E_2) \quad (3)$$
$$R_{\rm RR}(E_z, E_z') = \delta(E_z - E_z') - T_p \delta(E_z - E_1)\delta(E_z' - E_1). \quad (4)$$

The model (1)-(4) satisfies all the required symmetry properties, including unitarity. If, for a given energy E_z, we define $T_{\rm net} \equiv T_\rightarrow - T_\leftarrow$ where

$$T_\rightarrow(E_z) = \int dE_z' T_{\rm LR}(E_z, E_z') \quad , \quad T_\leftarrow(E_z) = \int dE_z' T_{\rm RL}(E_z, E_z'), \quad (5)$$

then we have [5]

$$T_{\rm net}(E_z) = T_p \left[\delta(E_z - E_2) - \delta(E_z - E_1)\right]. \quad (6)$$

A special property of our pump is that the ac driving is localized in space. Consequently, the distribution of *incident* electrons is not affected by the driving and can be taken to be in thermal equilibrium with the contact reservoirs. Furthermore, if we assume the temperature of the two contacts to be the same, and that no dc bias is applied, the distribution of incident electrons will be the same on both sides and given by a Fermi function $f(E-\mu)$, where μ is

the chemical potential in the contacts. With this the total current can simply be written as [5]

$$I = \int_{\Delta V}^{\infty} dE f(E-\mu) J(E) \tag{7}$$

$$J(E) = \frac{2e}{h} \int_{\Delta V}^{E} dE_z D_\perp(E-E_z) T_{\rm net}(E_z). \tag{8}$$

where $D_\perp$ is the density of states in the dimensions perpendicular to the direction of transport. In the single-pipeline model, Eqs. (6)–(8) yield

$$I = \frac{2e}{h} T_p \int_0^{\infty} dE_\perp D_\perp(E_\perp)[f(E_\perp + E_2 - \mu) - f(E_\perp + E_1 - \mu)]. \tag{9}$$

For one spatial dimension, Eq. (9) translates into

$$I_{\rm 1D} = \frac{2e}{h} T_p \left[f(E_2-\mu) - f(E_1-\mu) \right], \tag{10}$$

which has a peak at $\mu = (E_1+E_2)/2$, and an *exponential* decay for $\mu \gg kT$ as shown in panel B of Fig. 1. In 2D we find

$$I_{\rm 2D} \approx \frac{2e}{h^2} T_p \sqrt{2\pi m\beta} \Big[{\rm Li}_{-\frac{1}{2}}(-{\rm e}^{\beta\mu})(E_2-E_1) - \frac{\beta}{2} {\rm Li}_{-\frac{3}{2}}(-{\rm e}^{\beta\mu})(E_2^2 - E_1^2) \Big], \tag{11}$$

where Li is the polylogarithm function [11]. Expanding for $\mu \gg kT$ we find that in 2D the pump current decays only *algebraically* as $1/\sqrt{\mu}$. Finally, in 3D we obtain

$$I_{\rm 3D} \approx \frac{4\pi me}{h^3} T_p \left[f(-\mu)(E_1-E_2) + \frac{f'(-\mu)}{2}(E_1^2 - E_2^2) \right]. \tag{12}$$

For $\mu \gg kT$ one has $f(-\mu) \approx 1$ and $f'(-\mu) \approx 0$, i.e., the current in 3D becomes *independent* of μ in this limit, $I_{\rm 3D} = -(4\pi me/h^3) T_p (E_2 - E_1)$, as seen in panel B of Fig. 1. Thus we find the non-trivial result that the pump current does not necessarily decay with increasing chemical potential as one naively might expect.

III. SPECTRAL ANALYSIS

It is interesting to analyze the spectral function (8) that leads from Eq. (7) to Eq. (9). Within the single–pipeline model, one obtains

$$J(E) = \frac{2e}{h} T_p [D_\perp(E-E_2)\theta(E-E_2) - D_\perp(E-E_1)\theta(E-E_1)]. \tag{13}$$

Eq. (13) describes a function that is mainly localized in the pipeline region. In the particular case of three dimensions we have $D_\perp(E_\perp) = 2\pi m/h^2 \equiv D_0$ and Eq. (13) yields a square function localized between E_2 and E_1. Combining this result with Eq. (7), which tells us that the total electric current I is obtained by convoluting the spectral current density $J(E)$ with a thermal population of incoming electrons, we thus find that for $\mu \gg E_2$ the pump current is sustained by scattering states with incident energy well below the Fermi surface. An immediate consequence is that in this regime *the total pump current is insensitive to temperature*, even for $kT \sim \hbar\omega$. This remarkable result was noted in Ref. [5] and will be explored further in the following within the framework of the analytical single–pipeline model.

First we note that it is possible to perform sensible spectral decompositions of the current different from (7)-(8). In Eq. (7), the integration variable E refers to the *initial* electron energy. We may adopt an alternative viewpoint and write the current as an energy integral in which the variable E denotes not the initial but the *actual* energy of the electrons flowing through a given region, say, in the left lead.

From the single–pipeline model (1)-(4) we may write the pump current as

$$\begin{aligned} I &= \frac{2e}{h} \int dE_\perp \int dE_z \int dE_z' D_\perp(E_\perp) f(E_\perp + E_z - \mu) \\ &\quad \times [\delta(E_z - E_z') - R_{\rm LL}(E_z, E_z') - T_{\rm RL}(E_z, E_z')] \qquad (14) \\ &= \frac{2e}{h} \int dE_\perp \int dE_z \int dE_z' D_\perp(E_\perp) f(E_\perp + E_z - \mu) \\ &\quad \times T_p \left[\delta(E_z - E_2) - \delta(E_z - E_1) \right] \delta(E_z' - E_2). \qquad (15) \end{aligned}$$

We wish to analyze the total current in terms of the final energy $E = E_\perp + E'_z$ regardless of the initial longitudinal energy E_z [the term $\delta(E_z - E'_z)$ in Eq. (14) describing the contribution from the stream of incoming electrons is explicitly cancelled by an identical term in Eq. (3)]. With this goal in mind, we rewrite Eq. (15) as

$$\begin{aligned} I &= \frac{2e}{h} T_p \int_0^\infty dE \int_0^E dE_z D_\perp(E - E_z) \\ &\quad \times \left[f(E - E_z + E_2 - \mu) - f(E - E_z + E_1 - \mu) \right] \delta(E_z - E_2) \end{aligned} \tag{16}$$

to obtain $I = \int_0^\infty J_L(E)\, dE$, where

$$J_L(E) = \frac{2e}{h} T_p \theta(E - E_2) D_\perp(E - E_2) \left[f(E - \mu) - f(E - \hbar\omega - \mu) \right]. \tag{17}$$

In the 3D case, for which $D_\perp(E - E_2) = D_0$, it is clear that for $\mu \gg E_2$ the current spectrum in the left lead is essentially localized between μ and $\mu + \hbar\omega$, where we have taken $E_2 - E_1 = \hbar\omega$. A similar analysis for the current in the right lead yields $I = \int_{\Delta V}^\infty J_R(E)\, dE$ with

$$J_R(E) = \frac{2e}{h} T_p \theta(E - E_1) D_\perp(E - E_1) \left[f(E + \hbar\omega - \mu) - f(E - \mu) \right], \tag{18}$$

which tells us that, except for thermal smearing, the net current is carried by electrons with energies between $\mu - \hbar\omega$ and μ. We conclude that there is an average increase of $\hbar\omega$ in the energy of the electrons responsible for the current. This is expected, since $\hbar\omega$ is precisely the energy gained by electrons being transmitted from right to left. Thus we encounter the interesting result that, while the current is due to a lack of cancellation between scattering states with initial energies well below the Fermi level, the net current in the leads is carried by electrons near the Fermi surface. The energies of the independent electrons are modified in such a way that the current may have very different spectral properties depending on the way in which it is analyzed. The numerical results discussed in the next section [see Fig. 4] confirm these analytical predictions.

This result is exact but, perhaps, somewhat counterintuitive initially. One way of reconciling the two pictures is to try to understand them separately and to notice that they are, in fact, compatible.

(i) If we view the net current as resulting from a lack of cancellation between scattering states whose incident channel has total energy E, it is easy to interpret Eqs. (7) and (13): If $E < E_1$ no state can benefit from the pipeline, and hence there is no contribution to the current at these energies. For $E_1 < E < E_2$ only states coming from the right can take advantage of the pipeline and carry any current — therefore, clearly, $J(E) \neq 0$ here. On the other hand, if $E > E_1$, E_2, there will be channels incident from *both* sides, whose energy in z-direction, E_z, matches the pipeline. Since the current from each side depends on the available density of states in the transverse direction, $D_\perp(E - E_z)$, and secondly, as one must fulfill the matching conditions $E_z = E_2$ on the left and $E_z = E_1$ on the right, Eq. (13) is readily understood. In this picture we thus have to conclude that $J(E)$ is localized in the pipeline region and furthermore, as gathered from Eq. (7), that $J(E)$ is independent of the (common) distribution function in the contacts.

(ii) In the alternative picture put forward in the present work we focus on, say, the current density $J_{\rm L}(E)$ on the left-hand side of the pump. Now E refers to the local electron energy on that side, regardless of where the electron came from originally. It is clear that in this case the current results from a lack of cancellation between *left-going* electrons transmitted from the right-hand side via the pipeline, and therefore weighted with probability $f(E + E_1 - E_2 - \mu)$, and *right-going* transmitted electrons distributed according to $f(E - \mu)$. For a given energy $E > E_2$ the electrons contributing will be those that fulfill the pipeline-matching condition on the left-hand side, $E_z = E_2$, and their number will be proportional to the transverse density of states, $D_\perp(E - E_2)$. Hence the structure of Eq. (17), which yields a spectral function that is localized within $E_2 - E_1 = \hbar\omega$ of the Fermi surface. Note that, in contrast to the first case, this definition of a spectral current density does explicitly depend on the distribution function.

Yet, there is no contradiction between pictures (i) and (ii). A net current results from a lack of cancellation between current-carrying states, but the natural way to identify these states depends on the way we group them into cancelling pairs. This can be done in more than one sensible way, especially if the energy of the electron is not conserved. In (i) we compare *retarded scattering states* with initial energy E, whereas in (ii) we compare *scattering channels* of energy E on a given side of the pump. Both pictures are equally valid but, depending on the aspect one wishes to explain, one may favor one over the other.

An interesting feature is that, while the total current is essentially independent of temperature for $\mu - E_2 \gg kT$, the local spectral distributions J_L and J_R are indeed sensitive to temperature. This suggests the existence of an effective sum rule that eliminates the temperature dependence of Eqs. (17) and (18) when integrated over energy. It is easy to check this result explicitly in the 3D case, if one focuses on the limit $\omega \ll kT$. Then Eq. (18) can be approximated as

$$J_R(E) \approx (eT_p D_0/\pi)\, \omega f'(E + \hbar\omega/2 - \mu), \tag{19}$$

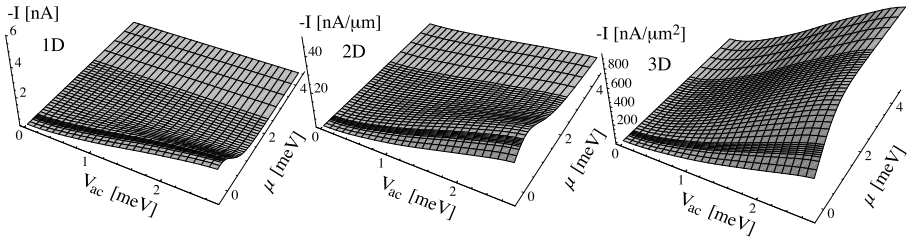

FIG. 2: Net pump current for 1, 2, and 3D at $T = 4.2$ K as a function of the driving amplitude $V_{\rm ac}$ and chemical potential μ. Parameters: $\hbar\omega = 0.1$ meV ≈ 24 GHz, $V_{\rm b} = 10$, $V_{\rm qw} = -4$, $\Delta V = -1$ (meV), $d_{\rm b} = 10$, $d_{\rm qw} = 12.5$ (nm).

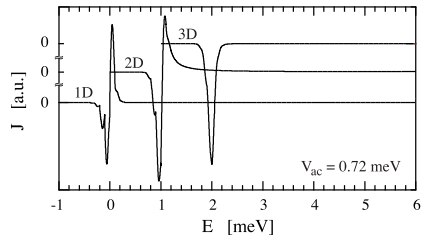

FIG. 3: Spectral current density $J(E)$ [see Eq. (7)] as function of the *total* energy of the incident electron, for 1, 2, and 3D. Curves are displaced for clarity. Parameters as in Fig. 2.

which yields a result manifestly independent of temperature when integrated over energy.

We end this section by noting two properties of the single–pipeline model. First, the left and right spectral functions can be shown to be exactly shifted by $\hbar\omega$,

$$J_L(E + \hbar\omega) = J_R(E), \tag{20}$$

which is a straightforward consequence of (17) and (18). Second, there is a reflection symmetry around the chemical potential: If all energies are with reference to μ,

$$J_L(E) = J_R(-E), \tag{21}$$

as long as $|E| < |E_2|$. This result is independent of the particular values of E_1 and E_2, and hence we expect it to survive in realistic situations with a continuous distribution of pipelines and higher-order energy transfers of $E_2 - E_1 = 2\hbar\omega, 3\hbar\omega, \ldots$. This expectation is confirmed by the numerical results presented below (see Fig. 4).

IV. NUMERICAL RESULTS

A full numerical analysis based on transfer matrices [12] fully confirms the results of the pipeline model: Figure 2 shows the results for the pump current as a function of driving strength $V_{\rm ac}$ and chemical potential μ at an elevated temperature of 4.2 K and a photon energy of $\hbar\omega = 0.1$ meV. The analytical results of the pipeline model of Fig. 1, panel B, are clearly identified in Fig. 2 when looking at cuts of constant driving amplitude $V_{\rm ac}$. This supports the initial observation [see Eq. (12)] that the pump current in 3D is largely independent of temperature, as long as $\mu - E_2 \gg kT$.

As discussed in Sect. III, the reason for this resilience against temperature can be most easily understood when considering the spectral current density. Let us first use the definition (8) for $J(E)$ based on incident channels. Figure 3 shows $J(E)$ in 1, 2, and 3D as a function of the total energy of the incident electron for $V_{\rm ac} = 0.72$ meV. As expected from the analytic discussion, in all cases do we find the largest contribution to the current stemming from states with small total kinetic energy close to the conduction band edge, although the details depend on the dimensionality of the pump. Consequently, for $\mu - E_2 \gg \hbar\omega$ the bulk of the pump current is carried by states far below the Fermi surface and is insensitive to changes in temperature, which afflict the shape of the distribution function at the Fermi surface only.

The numerical results shown in Fig. 3 for a realistic device are explained qualitatively by Eq. (13), further underlining the adequacy of the pipeline model used in [5]. In three-dimensions Eq. (13) yields a square function localized between

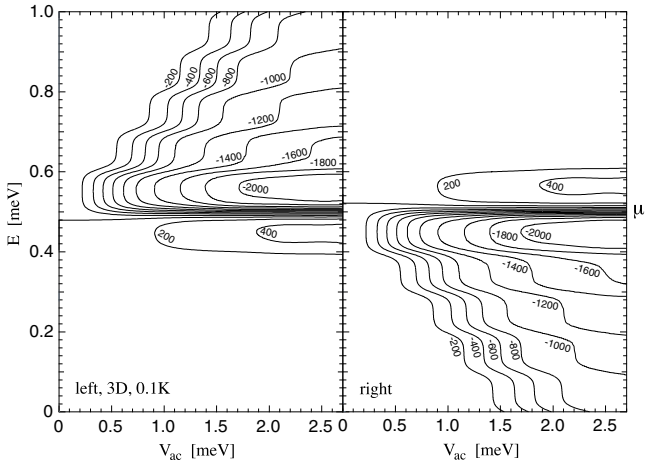

FIG. 4: Asymptotic spectral current densities (in nA/(μm^2 meV)) in the left and right contacts of a 3D pump with $\mu = 0.5\,\mathrm{meV}$, $T = 0.1\,\mathrm{K}$, $\hbar\omega = 0.1\,\mathrm{meV}$. Other parameters as in Fig. 2. 1D and 2D pumps have similar characteristics at low temperatures.

E_2 and E_1. The rounded peak shown in Fig. 3 for the three-dimensional case indicates that, in practice, one rather has a continuous distribution of pipelines.

As pointed out before, another useful definition of a spectral current density is based on the calculation of the net current in the leads. In this case we simply take the difference of the currents carried by the incident and outgoing channels on the same side. This is most conveniently done by adding all channels incoherently. We find that for temperatures low compared to the photon energy the current density is centred around the Fermi energy. Figure 4 shows the case of a 3D pump operated at the relatively low temperature of 0.1 K. The chemical potential was taken to be 0.5 meV, which is somewhat larger than the photon energy of 0.1 meV. On the right-hand side, the biggest contribution to the pump current stems from states about $\hbar\omega/2$ *below* the Fermi energy. These are then pumped across the barrier and end up at energies roughly $\hbar\omega/2$ *above* the Fermi energy on the left — indicating that the single most important process in the pump involves a single photon, net. Very similar results are found for pumps of 1 and 2 spatial dimensions. This agrees well with the analytical expectations from Eqs. (17) and (18). Fig. 4 also indicates that, for larger driving amplitudes, energy transfers of more than one photon quantum also contribute, although with a smaller weight. Finally, we note that the symmetry (21) around μ is very well satisfied in a realistic device, as expected from the analytic discussion.

V. CONCLUSIONS

We have presented a simple analytical model of electron transport through an asymmetric device driven by a local ac signal. The pipeline structure found in the electron transmission has its origin in the existence of a band offset between the two sides of the device. The analytic study yields an accurate understanding of the physics involved and shows good agreement with numerical results for a realistic case. A spectral analysis of the current reveals that the current is carried by electrons whose initial energy may be deep within the Fermi sea, making the pump effect resilient against temperature. On the other hand, the local spectral current density in the leads is localized near the Fermi surface.

We appreciate helpful discussions with S. Kohler. This work has been supported by the EU via TMR contract FMRX-CT98-0180, and by DGICyT (PB96-0080-C02).

[1] M. Switkes, C. M. Marcus, K. Campman, and A. C. Gossard. An Adiabatic Quantum Electron Pump. *Science*, 283:1905, 1999.

[2] D. J. Thouless. Quantization of particle transport. *Phys. Rev. B*, 27:6083, 1983. Q. Niu. Quantum adiabatic particle transport. *Phys. Rev. Lett.*, 64:1812, 1990. I. L. Aleiner and A. V. Andreev. Adiabatic Charge Pumping in Almost Open Dots. *Phys. Rev. Lett.*, 81:1286, 1998. F. Zhou, B. Spivak, and B. L. Altshuler. Mesoscopic Mechanism of Adiabatic Charge Transport. *Phys. Rev. Lett.*, 82:608, 1999. B. L. Altshuler and L. I. Glazman. Pumping Electrons. *Science*, 283:1864, 1999.

[3] C. A. Stafford and N. S. Wingreen. Resonant Photon–Assisted Tunneling through a Double Quantum Dot: An Electron Pump from Spatial Rabi Oscillations. *Phys. Rev. Lett.*, 76:1916, 1996. T. H. Stoof and Y. V. Nazarov. Time–dependent resonant tunneling via two discrete states. *Phys. Rev. B*, 53:1050, 1996. Mathias Wagner. Probing Pauli Blocking Factors in Quantum Pumps with broken Time-reversal Symmetry. *Phys. Rev. Lett.* 85:174, 2000.

[4] L. J. Geerligs *et al.*. Frequency-locked turnstile device for single electrons. *Phys. Rev. Lett.*, 64:2691, 1990. L. P. Kouwenhoven *et al.*. Quantized current in a quantum–dot turnstile using oscillating tunnel barriers. *Phys. Rev. Lett.*, 67:1626, 1991.

[5] M. Wagner and F. Sols. Subsea electron transport: Pumping deep within the Fermi sea. *Phys. Rev. Lett.*, 83:4377, 1999.

[6] M. O. Magnasco. Forced thermal ratchets. *Phys. Rev. Lett.*, 71:1477, 1993.

[7] R. Bartussek, P. Hänggi, and J. G. Kissner. Periodically rocked thermal ratchets. *Europhys. Lett.*, 28:459, 1994.

[8] I. Zapata, R. Bartussek, F. Sols, and P. Hänggi. Voltage rectification by a SQUID ratchet. *Phys. Rev. Lett.*, 77:2292, 1996. I. Zapata, J. Łuczka, F. Sols, and P. Hänggi. Tunneling center as a source of voltage rectification in Josephson junctions. *Phys. Rev. Lett.*, 80:829, 1998.

[9] P. Reimann, M. Grifoni, and P. Hänggi. Quantum ratchets *Phys. Rev. Lett.*, 79:10, 1997.

[10] M. H. Pedersen and M. Büttiker. Scattering theory of photon–assisted electron transport. *Phys. Rev. B*, 58:12993, 1998.

[11] L. Lewin. *Polylogarithms and Associated Functions*, (North Holland, New York, 1981).

[12] M. Wagner. Photon-assisted transmission through an oscillating quantum well: A transfer-matrix approach to coherent destruction of tunneling. *Phys. Rev. A*, 51:798, 1995.